

Molecular simulation of supercritical water and aqueous solutions

This article has been downloaded from IOPscience. Please scroll down to see the full text article.

1996 J. Phys.: Condens. Matter 8 9281

(<http://iopscience.iop.org/0953-8984/8/47/016>)

View [the table of contents for this issue](#), or go to the [journal homepage](#) for more

Download details:

IP Address: 171.66.16.207

The article was downloaded on 14/05/2010 at 04:31

Please note that [terms and conditions apply](#).

Molecular simulation of supercritical water and aqueous solutions

Peter T Cummings and Ariel A Chialvo

Department of Chemical Engineering, University of Tennessee, Knoxville, TN 37996-2200, USA
and Chemical Technology Division, Oak Ridge National Laboratory, Oak Ridge, TN 37831-6268, USA

Received 15 July 1996

Abstract. We describe molecular dynamics simulations of supercritical water and supercritical aqueous solutions using simple non-polarizable models of water and a new polarizable model for water developed by our research group. We compare the simulation results to neutron diffraction studies where available and to experimental measurements of ion pairing in the case of supercritical aqueous electrolyte solutions. Simulation results obtained on massively parallel supercomputers are used to evaluate size effects in the simulations and to speed up the CPU-time-consuming polarizability component of the simulation.

1. Introduction

For over a decade, our research group has been interested in understanding the properties of aqueous solutions, particularly supercritical water, supercritical aqueous electrolyte solutions and ambient pressure phase equilibria of mixed solvent electrolyte systems (systems consisting of an electrolyte dissolved in a solvent consisting of water and another non-electrolyte species). Our approach to these systems has been a combination of experiment [1–3], molecular theory [4–6], and molecular simulation [7–18].

During the past two decades, supercritical fluids have generated considerable interest because of their application as solvents in supercritical solvent extraction processes, in supercritical fluid chromatography and as reaction media. The unique combination of the dissolving power of a liquid combined with the transport properties of a gas and the ability to cause large density changes with small pressure and/or temperature changes are the main reasons for much of the interest in supercritical fluids and their mixtures. In particular, supercritical water and supercritical aqueous solutions have been the subject of intense scrutiny due to increasing interest in the use of supercritical water as the solvent for oxidation of organic wastes (supercritical water oxidation). Unlike ambient water, supercritical water is a good solvent for organic species and a poor solvent for ionic species (such as electrolytes) and gases (such as oxygen). In the latter case, the low solubility of ionic species is related to the high degree of ion pairing present in supercritical aqueous electrolyte solutions.

In this paper, we describe our recent work on supercritical water and supercritical aqueous electrolyte solutions. New results on ion-pairing in supercritical aqueous electrolyte solutions are presented.

2. Supercritical water

An important issue in the modelling of supercritical aqueous solutions is the degree of hydrogen bonding present. Recent neutron diffraction with isotopic substitution (NDIS) experiments on supercritical water [19,20] have led to the suggestion that hydrogen bonding is absent from supercritical water at temperatures above 673 K on the basis of the disappearance of the ‘hydrogen-bonding’ peak from the oxygen–hydrogen radial distribution function, $g_{OH}(r)$, located at approximately 1.8 Å. These findings have been challenged both by experimental [21] and by simulation studies [15,22–24]. In particular, Chialvo and Cummings [15] pointed out that the SPCG model, a simple modification of the non-polarizable simple point charge (SPC) model for water [25] consisting of re-scaling the dipole moment of the model (2.27 D) to that of the isolated water molecule (1.85 D), predicts a $g_{OH}(r)$ in much better agreement with NDIS data. Specifically, the SPCG model does not exhibit the ‘hydrogen-bonding peak’ under supercritical conditions. However, even in the absence of the ‘hydrogen-bonding peak’, this model predicts a considerable degree of hydrogen bonding at supercritical states, as shown in figure 1. Chialvo and Cummings concluded that the orientationally averaged nature of $g_{OH}(r)$ renders it a poor indicator of the degree of hydrogen bonding in supercritical water.

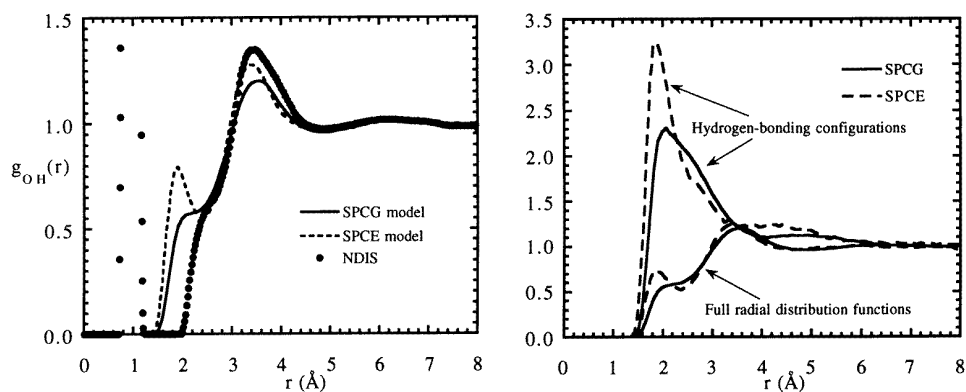


Figure 1. Left: a comparison between the experimental and the simulated SPCE [26] and SPCG O–H radial distribution functions of water at $\rho = 0.66 \text{ g cm}^{-3}$ and $T = 673 \text{ K}$. Right: a comparison between the radial and hydrogen-bonding components of the O–H distribution functions for the SPCE and SPCG water models under the same conditions.

Chialvo and Cummings [27] conducted a comprehensive study of the popular rigid non-polarizable point-charge models and concluded that non-polarizable models, fitted to the ambient conditions properties of liquid water, cannot be expected to provide accurate predictions of thermophysical properties and structure over wide ranges of density and temperature, in the supercritical regime in particular. This is consistent with observations based on phase equilibria [11]. Although many polarizable models exist in the literature, few have the property of reducing to the bare dipole moment of water at zero density, which we regard as very important in order to model the supercritical regime. Therefore, we have undertaken the development of an intermolecular potential for water which has this property. In the first version of this model [28] electrostatic charges were initially located on the three SPC sites, with magnitudes such that the permanent dipole moment is that of the isolated water molecule, 1.85 D. We analysed the situation for which the negative

charge is located along the H–O–H bisector at a distance R_{OM} towards the H sites while preserving the permanent dipole moment of 1.85 D. With this geometry, the model consists of a Lennard-Jones O–O pair plus the M–M and M–H electrostatic pair interactions. In addition, we include an isotropic–linear point dipole polarizability at the centre of mass (or at the O-site) to account for the many-body polarizability effects. Good agreement with measured NDIS results under ambient conditions was obtained for $0.1 \text{ \AA} \leq R_{OM} \leq 0.2 \text{ \AA}$. For $R_{OM} = 0.2 \text{ \AA}$ very good agreement with the bare quadrupole moment of water is obtained. Under supercritical conditions, the polarizable model is in better agreement with NDIS results than are the SPC and SPC/E models, as shown in figure 2 (especially the position of the first peak of $g_{OH}(r)$ is better than that of the SPC/E model). The total dipole moment decreases from $2.92 \pm 0.02 \text{ D}$ under ambient conditions to $2.4 \pm 0.1 \text{ D}$ (in remarkably good agreement with the *ab initio* simulation result of $2.3 \pm 0.2 \text{ D}$ [30]), with a polarization energy decreasing from -4.42 ± 0.2 to $-1.59 \pm 0.1 \text{ kcal mol}^{-1}$. This total dipole moment compares very well with the effective (permanent) dipole moment of the SPC/E model, 2.35 D. Interestingly, the PPC model of Kusalik and Svishchev [29], with a permanent dipole moment of 2.14 D, predicts not only a structure very similar to that of the proposed model (see figure 2) but also a total dipole moment of $2.38 \pm 0.05 \text{ D}$. Currently, we are working on an improved version of this model that features a smeared form of the point charges. Preliminary studies suggest that this step further improves the quantitative accuracy of the model under ambient conditions.

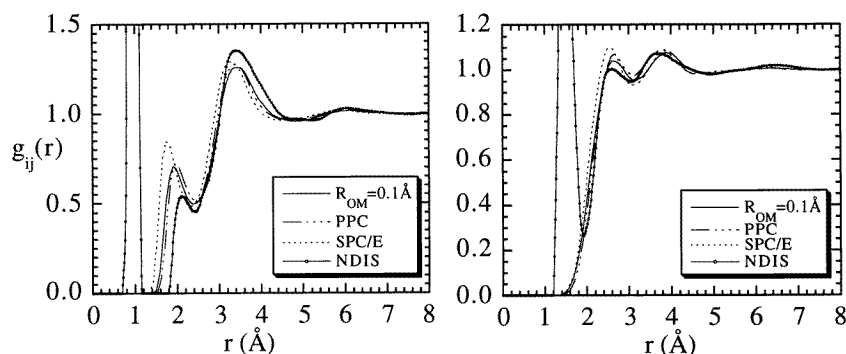
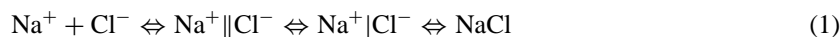


Figure 2. A comparison between the experimental NDIS and the simulated O–H (left) and H–H (right) radial distribution functions of water using the polarizable model with $R_{OM} = 0.1 \text{ \AA}$ at 573 K and 0.72 g cm^3 . PPC indicates the polarizable point charge model of Kusalik and Svishchev [29].

3. Ion-pairing in supercritical aqueous electrolyte solutions

In order to understand ion pairing in dilute supercritical aqueous solutions, we have undertaken a programme of molecular dynamics simulations of dilute aqueous NaCl solutions in near-critical water, particularly focusing on the Na^+/Cl^- association process which can be envisioned as



where NaCl is the product of the ‘reaction’ between the Na^+ and Cl^- ions, and $\text{Na}^+ \parallel \text{Cl}^-$ and $\text{Na}^+ | \text{Cl}^-$ represent the solvent-separated ion pair (SSIP) and contact ion pair (CIP)

states, respectively. Experimental evidence indicates that these two ion-paired states might act as reaction intermediates [31–35]. We determine the anion–cation potential of mean force by molecular dynamics simulation [18] complementing other results at higher temperature [36,37] and under ambient conditions [38]. Technical details of the simulation have been provided elsewhere [17]. The water–water interactions were described by the simple point charge (SPC) model of Berendsen *et al* [25], the ion–water interactions were modelled using the Pettitt–Rosky model [39] and for the ion–ion interaction we used the Fumi–Tosi model for alkali–halide interactions [40,41]. All simulations were performed with the ions at ‘infinite dilution’ in the isokinetic–isochoric ensemble, with $N = 256$ molecules, $N - 2$ water molecules plus an anion and a cation. The method used to calculate the anion–cation potential of mean force $W_{NaCl}(r)$ is the constraint technique of Ciccotti *et al* [42]. The NaCl radial distribution function at infinite dilution is calculated by $g_{NaCl}^{\infty}(r) = \exp[-W_{NaCl}(r)/(k_B T)]$, where k_B is Boltzmann’s constant and T is the absolute temperature. The equilibrium constants can be evaluated from $g_{NaCl}(r)$ [18]. The simulations were performed for state conditions corresponding to $(\rho_r, T_r) = (\rho/\rho_c, T/T_c) = (1.0, 1.05), (1.0, 1.2), (1.0, 1.4), (1.5, 1.05)$ and $(2.0, 1.05)$ based on the critical conditions for the SPC water model [9]. Standard periodic boundary conditions were used together with the minimum image criterion and a spherical cut-off with reaction field for the truncated intermolecular interactions [43]. The accuracy of the reaction field was assessed by performing Ewald summation simulations for a few typical constrained configurations [18]. The production runs for thermodynamic and structural properties comprised 3×10^4 time steps (30 ps) whereas those for mean-force calculations were extended to 10^5 time steps for each constrained ion-pair distance. Despite the inadequacies of non-polarizable models noted in section 2, the thermodynamic properties of the SPC model in supercritical states are predicted quite accurately for corresponding states (the same $\rho_r = \rho/\rho_c$ and $T_r = T/T_c$), as shown by Cummings *et al* [8].

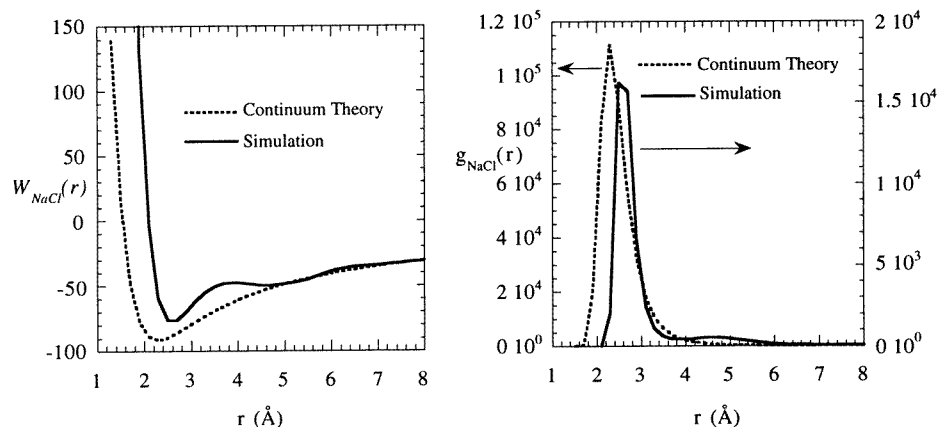


Figure 3. The potential of mean force (left) and the radial distribution function (right) between sodium and chloride ions at infinite dilution in supercritical water ($T_r = 1.05$, $\rho_r = 1.0$) calculated by simulation (—) and using the continuum theory given by equation (2).

The potential of mean force and the NaCl radial distribution function at infinite dilution at $T_r = 1.05$ and $\rho_r = 1.0$ are shown in figure 3. The simulation results are compared to the continuum theory in which the potential of mean force is assumed to be given by the bare

potential between the ions, $u_{NaCl}(r)$, screened by the dielectric constant of the solvent, ϵ ,

$$W_{NaCl}^{continuum}(r) = u_{NaCl}^{Non-Coulombic} + \frac{u_{NaCl}^{Coulombic}}{\epsilon}. \quad (2)$$

The equilibrium constant for association is given by

$$K_a^M = \frac{\rho_{CIP} + \rho_{SSIP}}{\rho_{Na^+} \rho_{Cl^-}} \quad (3)$$

where the superscript M denotes units of $l \text{ mol}^{-1}$ and ρ_{SSIP} , ρ_{CIP} , ρ_{Na^+} and ρ_{Cl^-} are the densities of solvent-separated ion pairs, contact ion pairs, unassociated Na^+ ions and unassociated Cl^- ions respectively while the equilibrium between SSIP and CIP is given by

$$K_e = \frac{\rho_{SSIP}}{\rho_{CIP}}. \quad (4)$$

To eliminate uncertainties associated with the calculation of the dielectric constant of the SPC model, it turns out to be more appropriate to consider the related quantity $I_a = K_a^M \exp[q_{Na}q_{Cl}/(\epsilon r_0 k_B T)]$, where q_a is the charge on ion α , $\alpha = Na^+$ or Cl^- . This quantity is a very sensitive function of the state conditions. For example, simulation results indicate that $\log I_a \approx 4.3$ at $\rho = 0.1252 \text{ g cm}^3$ and $T = 800 \text{ K}$ [37], $\log I_a \approx 5.6$ at $\rho = 0.0832 \text{ g cm}^3$ and $T = 800 \text{ K}$ [37], and $\log I_a \approx -1.38$ under ambient conditions [38]. For the state points under consideration here, the simulation predictions are given in table 1 together with experimental results. As previously shown [18, 44], at $(\rho_r, T_r) = (1.0, 1.05)$ the experimental and simulation values are within the uncertainty of each quantity. This is remarkably good agreement given both the difficulties of the experimental measurement and the various approximations involved in the simulation model. As is clear from the remainder of the entries in table 1, and from figure 4, this agreement does not persist to higher densities or temperatures, although given the range of values of I_a , the agreement is still quite impressive given that none of the intermolecular potentials has been fitted to any experimental data at supercritical conditions, let alone the ionic association equilibrium. The failure at higher temperatures and densities can be traced largely to the inadequacy of the dielectric constant predictions of SPC in these states.

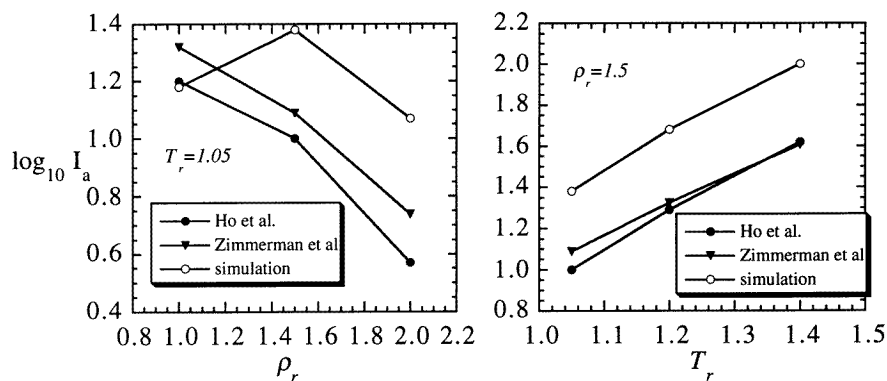


Figure 4. Simulation results for the isochoric temperature-dependence (left) and the isothermal density-dependence (right) of the ion-pair association constant I_a in comparison with the corresponding conductance experimental data of Ho *et al* [44] and Zimmerman *et al* [45].

Table 1. Simulation results for $\log I_a$ as a function of the state conditions.

	$\rho_r = 1.0$	$\rho_r = 1.5$	$\rho_r = 2.0$
$T_r = 1.05$	1.18 ± 0.04	1.38 ± 0.03	1.07 ± 0.03
$T_r = 1.20$		1.68 ± 0.04	
$T_r = 1.40$		2.00 ± 0.04	

4. Conclusions

Using intermolecular potentials taken from the literature, we have been able to conduct studies of supercritical water and supercritical aqueous solutions which provide insight into the physical basis for the properties of these intriguing and practical systems. Further quantitative accuracy will require more accurate intermolecular potentials, particularly including polarizability effects in the water potential. This is the current focus of our research efforts.

Acknowledgments

This work was supported by the Division of Chemical Sciences, Office of Basic Energy Sciences, USA Department of Energy. Some of the computations reported in this work were performed on the IBM RS/6000 in the Computational Laboratory for Environmental Biotechnology in the Department of Chemical Engineering at the University of Virginia. The authors also acknowledge the collaboration of colleagues Hank Cochran, Mike Simonson and Bob Mesmer in parts of the work reported here and fruitful discussions with Igor Svishchev and Peter G Kusalik on molecular dynamics simulations of polarizable models for water.

References

- [1] Morrison J F, Baker J C, Meredith H C, Newman K E, Walter T D, Massie J D, Perry R L and Cummings P T 1990 *J. Chem. Eng. Data* **35** 395
- [2] Slusher J T, Decker K J, Liu H, Vega C A, Cummings P T and Oconnell J P 1994 *J. Chem. Eng. Data* **39** 506–9
- [3] Slusher J T, Cummings P T, Hu Y Q, Vega C A and Oconnell J P 1995 *J. Chem. Eng. Data* **40** 792–8
- [4] Perry R L, Massie J D and Cummings P T 1987 *Fluid Phase Equilibria* **39** 227
- [5] Chialvo A A and Cummings P T 1994 *AIChE J.* **40** 1558–73
- [6] Chialvo A A, Kalyuzhnyi Y V and Cummings P T 1996 *AIChE J.* **42** 571–84
- [7] Strauch H J and Cummings P T 1989 *Molec. Simulation* **2** 89–104
- [8] Cummings P T, Cochran H D, Simonson J M, Mesmer R E and Karaborni S 1991 *J. Chem. Phys.* **94** 5606–21
- [9] de Pablo J J, Prausnitz J M, Strauch H J and Cummings P T 1991 *J. Chem. Phys.* **93** 7355–9
- [10] Cochran H D, Cummings P T, Karaborni S 1992 *Fluid Phase Equilibria* **71** 1–16
- [11] Strauch H J and Cummings P T 1992 *J. Chem. Phys.* **96** 864–5
- [12] Chialvo A A and Cummings P T 1993 *Molec. Simulation* **11** 163–75
- [13] Strauch H J and Cummings P T 1993 *Fluid Phase Equilibria* **86** 147–72
- [14] Chialvo A A, Cummings P T and Cochran H D 1996 *Int. J. Thermophys.* **17** 147–56
- [15] Chialvo A A and Cummings P T 1994 *J. Chem. Phys.* **101** 4466–9
- [16] Cummings P T, Chialvo A A and Cochran H D 1994 *Chem. Eng. Sci.* **49** 2735–48
- [17] Chialvo A A, Cummings P T, Cochran H D, Simonson J M and Mesmer R E 1995 *Supercritical Fluid Science and Technology* ed N Foster and K W Hutchenson (Washington: American Chemical Society)
- [18] Chialvo A A, Cummings P T, Cochran H D, Simonson J M and Mesmer R E 1995 *J. Chem. Phys.* **103** 9379–87

- [19] Postorino P, Tromp R H, Ricci M-A, Soper A K and Neilson G W 1993 *Nature* **366** 668–70
- [20] Tromp R H, Postorino P, Neilson G W, Ricci M A and Soper A K 1994 *J. Chem. Phys.* **101** 6210–5
- [21] Gorbaty Y E and Kalinichev A G 1995 *J. Phys. Chem.* **99** 5336–40
- [22] Loffler G, Schreiber H and Steinhauser O 1994 *Ber. Bunsenges. Phys. Chem.* **98** 1575–8
- [23] Kalinichev A G and Bass J D 1994 *Chem. Phys. Lett.* **231** 301–7
- [24] Kalinichev A G and Heinzinger K 1995 *Geochim. Cosmochim. Acta* **59** 641–50
- [25] Berendsen H J C, Postma J P M, von Gunsteren W F and Hermans J 1981 *Intermolecular Forces: Proc. Fourteenth Jerusalem Symp. on Quantum Chemistry and Biochemistry* ed B Pullman (Dordrecht: Reidel) pp 331–42
- [26] Berendsen H J C, Grigera J R and Straatsma T P 1987 *Phys. Chem.* **91** 6269–71
- [27] Chialvo A A and Cummings P T 1996 *J. Phys. Chem.* **100** 1317–22
- [28] Chialvo A A and Cummings P T 1996 *J. Chem. Phys.* **105** at press
- [29] Kusalik P G and Svishchev I M 1994 *Science* **265** 1219–21
- [30] Fois E S, Sprik M and Parrinello M 1994 *Chem. Phys. Lett.* **223** 411–15
- [31] Fleissner G, Hallbrucker A and Mayer E 1993 *J. Phys. Chem.* **97** 4806–14
- [32] Hage W, Hallbrucker A and Mayer E 1992 *J. Phys. Chem.* **96** 6473–88
- [33] Spohn P D and Brill T B 1989 *J. Phys. Chem.* **93** 6224–31
- [34] Winstein S, Clippinger E, Fainberg A H and Robinson G C 1954 *J. Amer. Chem. Soc.* **76** 2597–8
- [35] Sadek H and Fuoss R M 1954 *J. Amer. Chem. Soc.* **76** 5905
- [36] Gao J L 1994 *J. Phys. Chem.* **98** 6049–53
- [37] Cui S and Harris J G 1994 *Chem. Eng. Sci.* **49** 2749–63
- [38] Guardia E, Rey R and Padro J A 1991 *Chem. Phys.* **155** 187–95
- [39] Pettitt B M and Rosky P J 1986 *J. Chem. Phys.* **84** 5836–44
- [40] Fumi F G and Tosi M P 1964 *J. Phys. Chem. Solids* **25** 31
- [41] Tosi M P and Fumi F G 1964 *J. Phys. Chem. Solids* **25** 45
- [42] Ciccotti G, Ferrario M, Hynes J T and Kapral R 1989 *Chem. Phys.* **129** 241–51
- [43] Allen M P and Tildesley D J 1987 *Computer Simulation of Liquids* (Oxford: Oxford University Press)
- [44] Ho P C, Palmer D A and Mesmer R E 1994 *J. Solution Chem.* **23** 997–1018
- [45] Zimmerman G H, Gruszkiewicz M S and Wood R H 1995 *J. Phys. Chem.* **99** 11 612–25